

Observational Models of Graphite Pencil Materials

Mario Costa Sousa[†] and John W. Buchanan[‡]

[†] Department of Computing Science, University of Alberta, Edmonton, AB, Canada, T6G 2H1
mario@cs.ualberta.ca

[‡] Research Scientist at Electronic Arts (Canada), Inc.
4330 Sanderson Way, Electronic Arts Centre, Burnaby, B.C., Canada V5G 4X1
juancho@ea.com

Abstract

This paper presents models for graphite pencil, drawing paper, blenders, and kneaded eraser that produce realistic looking pencil marks, textures, and tones. Our models are based on an observation of how lead pencils interact with drawing paper, and on the absorptive and dispersive properties of blenders and erasers interacting with lead material deposited over drawing paper. The models consider parameters such as the particle composition of the lead, the texture of the paper, the position and shape of the pencil materials, and the pressure applied to them. We demonstrate the capabilities of our approach with a variety of images and compare them to digitized pencil drawings. We also present image-based rendering results implementing traditional graphite pencil tone rendering methods.

Keywords: Non-photorealistic rendering, natural media simulation, tone and texture, pencil rendering, image-based rendering, illustration systems.

1. Introduction

The display of models using highly realistic illumination models has driven much of the research in computer graphics. Researchers in non-photorealistic rendering (NPR) seek to provide alternative display methods for 3D models or 2D images. Particularly, recent work has focused on the modeling of traditional artistic media and styles such as pen-and-ink illustration^{6, 7} and watercolor paintings^{4, 13}. By providing rendering systems that use these alternative display models users can generate traditional renderings. These systems are not intended to replace artists or illustrators, but rather to provide a tool for users with no training in a particular medium, thus enabling them to produce traditional images.

In this paper we present results from our research in pencil illustration methods for NPR. The main motivation for this work is to investigate graphite pencil as a useful technical and artistic NPR production technique to provide alternative display models for users. We chose the pencil because it is a flexible medium, providing a great variety of styles of line quality, hand gesture, and tone building. It is excellent for preparatory sketches

and for finished rendering results. Pencil renderings are used by many people in different contexts such as scientific and technical illustration, architecture, art and design.

Our approach was to break the problem of simulating pencil drawings down into the following sub-problems:

1. Drawing materials: low-level simulation models for wood-encased graphite pencil and drawing paper, and for blenders and kneaded eraser¹⁷.
2. Drawing primitives: pencil stroke and mark-making (for tones and textures) built on top of the drawing materials¹⁸.
3. Rendering methods built on top of the drawing primitives. Algorithms for outlining, shading, shadowing, and texturing of reference images¹⁷ and 3D objects with a look that emulates real pencil renderings¹⁸.
4. High-level tools: partial control of the drawing composition through ordering and repeating of drawing steps¹⁸.

In this paper we present in detail the modeling of the drawing materials (sub-problem 1).

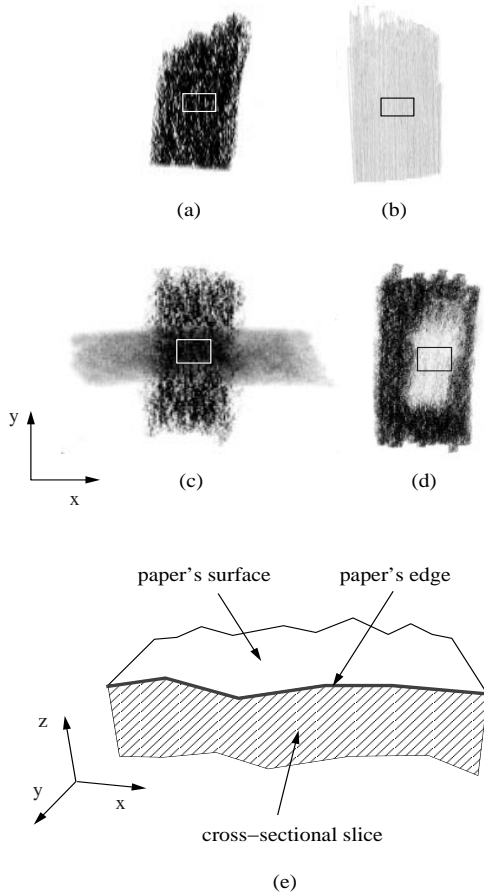


Figure 1: Sampled rectangular areas from real pencil work. Each sample was magnified by an electron scanning microscope (SEM) producing aerial and cross-sectional image results: A medium weight, moderate tooth drawing paper was used (Figure 6) with (a) soft pencil (Figure 8), (b) hard pencil (Figure 9), (c) blender (Figure 18), and (d) kneaded eraser (Figure 17). The diagram in (e) shows the viewing position for the SEM cross-sectional views of the samples (right image on Figures 6, 8, 9, 17, 18).

The models in this paper can be adapted to existing interactive illustration systems^{2, 5, 6} and 3D NPR systems for technical illustration, art, and design^{3, 7, 8, 9, 10, 12, 15, 16}. We have adapted our pencil and paper model to render 3D objects automatically using traditional pencil illustration and rendering methods¹⁸.

1.1. Related Work

Our pencil and paper model is based on the graphite, clay, and wax composition of the pencil lead and on the

texture and weight of the paper. Our blender and eraser model is based on their absorptive and dispersive properties of deposited lead material (graphite, clay, and wax particles) on drawing paper. We also considered most of the effects that are important for a pencil illustrator to master, particularly the order in which pencil materials are used, the pressure applied, the manner in which the pencil materials are shaped and held. Previous work on pencil simulation has addressed few of these issues. Vermeulen and Tanner² introduced a simple pencil model as part of an interactive painting system that does not include a model to handle textured paper and other supplementary drawing materials. Takagi and Fujishiro¹⁴ presented a model for paper micro-structure and pigment distribution for colored pencils to be used in digital painting. In the commercial realm, some interactive painting systems such as Fractal Design Painter[†] offer pencils, erasers, and blenders models with some interaction with the paper. Our models improve the approximation of graphite pencil renderings on drawing paper.

1.2. Overview

The organization of this paper is as follows. Section 2 describes the observational approach taken to build our models. Section 3 presents in detail the pencil model and Section 4 presents the paper model. The interaction between the two models is described in Section 5. Section 6 presents the blender and eraser model. The interaction of blenders and erasers with the pencil and paper model is described in Section 7. Section 8 presents results from our models on different paper textures, various pencil swatches (tone samples), and on tone rendering methods.

2. The Observational Approach

Our approach is based on an observational model of the interaction among real graphite pencil drawing materials (pencil, paper, eraser, blender). The goal was to capture the essential physical properties and behaviors observed to produce quality pencil marks at interactive rates. Our intention was not to develop a highly physically accurate model, which would lead to a computationally expensive simulation. All parameters described are important to achieve good pencil simulation results. The observations were performed by producing a great variety of pencil/blender/eraser swatches, strokes, and marks over different types of drawing papers, and magnifying them by using the Hitachi S-2700 scanning electron microscope (SEM) from the Department of Chemical

[†] Although some systems offer “pencil” mode it is difficult to determine what physical model, if any, is being used to simulate the pencil, blenders, and erasers.

Pencil model	
P_d	Pencil degree of hardness (Subsection 3.1, Table 2).
G_p, C_p, W_p	Percentage values of the mass amount of graphite, clay, and wax particles (Subsection 3.1, Table 2).
L_t	Lead thickness (Subsection 3.1).
T_s	Tip shape (Subsection 3.2.1, Figure 2).
P_c	Pressure distribution coefficients (Subsection 3.2.2, Figure 3).
Paper model	
w	Paper weight (Section 4).
F_s	Total amount of lead material to fill the surface of the grain (Subsection 5.4).
F_v	Total amount of lead material to fill the volume of the grain (Subsection 5.4).
V_g	Grain porous threshold volume (Subsection 5.4, Equation 3, Figure 5(b)).
T_v	Lead threshold volume (Subsection 5.4, Equation 4, Figure 11).
<i>Variables at paper(x,y) indexed by k, where k ∈ [1,4] :</i>	
h_k	Height of the grain (Section 4, Figure 5(a)).
L_k	Lead threshold volume (Subsection 5.4.1, Equation 5, Figure 11).
D_k	Percentage of lead material distributed (Subsection 5.4.1, Equation 6, Figure 11).
Pencil and paper interaction	
p	Pressure applied to the pencil (Subsection 5.3).
p'_c, p'_c	Pencil pressure at the pressure distribution coefficients P_c (Subsection 5.3, Equation 1, Figure 10).
(x_s, y_s, p_s)	Interpolated coordinates and pressure at the tip shape T_s (Subsection 5.3, Figure 10).
P_a	Averaged pencil pressure (Subsection 5.3).
D_l	Depth of lead into the grain (Subsection 5.5, Equation 7, Figures 12, 13).
B_v	Volume of lead bitten by the grain (Subsection 5.5, Equations 8, 9, 11).
h_m	Medium grain height (Subsection 5.5, Equation 10).
M	Percentage of extra lead material (Subsection 5.5, Equation 13).
<i>Variables at paper(x,y) indexed by k, where k ∈ [1,4] :</i>	
B_k	Volume of lead bitten (Subsection 5.5, Equations 12, 13).
(G_k, C_k, W_k)	Amount of graphite, clay, and wax deposited (Subsection 5.5, Equation 14).
T_k	Total amount of lead material deposited (Subsection 5.5, Equation 15).
E_k	Amount of paper damaged (Subsection 5.6, Equation 16).
A_k	Amount of graphite deposited (Subsection 5.7, Equation 18).
F_t	Maximum amount of lead material (Subsection 5.7).
I_k	Reflected intensity of lead material (Subsection 5.7, Equation 19).

Table 1: List of variables used for the pencil and paper model.

and Materials Engineering at the University of Alberta. These images were used to aid in the development of the observational models for pencils, papers, blenders, and erasers. Aerial and cross-sectional SEM images from real pencil drawing samples (Figure 1) were generated at 10kv accelerating voltage, with different magnifications, and with scale resolution in microns (see Figures 6, 8, 9, 17, 18).

3. Graphite Pencils

Our pencil model is from the category of wood-encased artist-grade graphite pencils²⁵. It has two main aspects:

the degree of hardness and softness and the kinds of sharpened points. They are described in the next subsections. A list of variables used throughout this section is given in Table 1.

3.1. Hard and Soft Pencils

Every pencil contains a writing core (or “lead”) which is made from a mixture of graphite, wax, and clay, the latter of which is the binding agent. The hardness of the lead depends on the percentage amount of graphite and clay. The more graphite it contains the softer and the thicker it is. Pencil hardness is graded in degrees

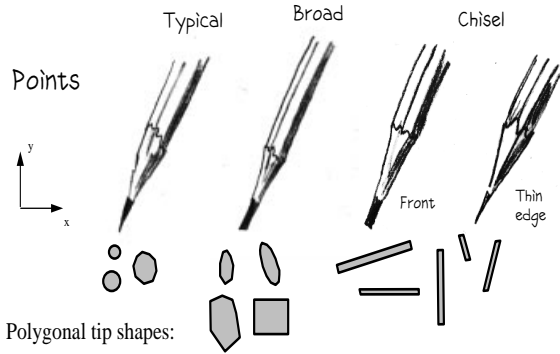


Figure 2: Different kinds of canonical points²⁰ and their polygonal tip shapes.

P_d . Usually, nineteen degrees is used ranging from 9H to 8B. The wax is included for lubrication. Table 2 presents the percentage values of the mass amount of graphite, clay, and wax particles for the nineteen grades of pencil. The thickness for a particular lead degree L_t is approximated by linearly interpolating between the thickness of the hardest lead (2 mm for 9H) and the thickness of the softest lead (4 mm for 8B).

3.2. Pencil Points

Sharpening a pencil in different ways changes the shape of the contact surface between the pencil and the paper. The pencil responds rapidly to almost any demand. Sharply pointed, it gives a line as fine and clean-cut as that of the pen; bluntly pointed, it can be used much like the brush. A pencil point is defined by tip shape and pressure distribution coefficients over the point's surface.

3.2.1. Tip Shape

The tip shape is defined as a polygonal outline based on the shape of three canonical types of sharpened pencil points (typical, broad, and chiseled)²⁰ (see Figure 2). A pencil tip shape is defined as $T_s = \{(x_i, y_i), s : 3 \leq i \leq n\}$, where (x_i, y_i) is one the n vertices of the polygon and s is the scale factor of the polygon used to account for the thickness of the lead.

3.2.2. Pressure Distribution Coefficients

Pressure distribution coefficients are values between 0 and 1 representing the percentage of the pencil's point surface that, on average, makes contact with the paper. This value is used to locally scale the pressure being applied to the pencil. The pressure distribution coefficients are defined as $P_c = (c, x, y), (c_i, x_i, y_i) : 1 \leq i \leq n\}$ where c is the value of the main pressure distribution coefficient whose location (x, y) can be anywhere within the polygon defining the tip shape (default location is

Pencil Number	Graphite	Clay	Wax
9H	0.41	0.53	0.05
8H	0.44	0.50	0.05
7H	0.47	0.47	0.05
6H	0.50	0.45	0.05
5H	0.52	0.42	0.05
4H	0.55	0.39	0.05
3H	0.58	0.36	0.05
2H	0.60	0.34	0.05
H	0.63	0.31	0.05
F	0.66	0.28	0.05
HB	0.68	0.26	0.05
B	0.71	0.23	0.05
2B	0.74	0.20	0.05
3B	0.76	0.18	0.05
4B	0.79	0.15	0.05
5B	0.82	0.12	0.05
6B	0.84	0.10	0.05
7B	0.87	0.07	0.05
8B	0.90	0.04	0.05

Table 2: Percentage values of the mass amount of graphite, clay, and wax particles for the entire range of pencil grades based on information received from pencil manufacturers.

at the center of the polygon), and c_i is the value of the pressure distribution coefficient at vertex (x_i, y_i) from the polygonal tip shape. Different values can be assigned to c and to each c_i . The closer they are to 1.0, the more surface is in contact with the paper. The closer they are to 0.0, the less surface is in contact with the paper. The values between c and c_i are computed by linear interpolation, thus defining the general shape of the pencil's tip (see Figure 3).

4. Drawing Papers

Good pencils are essential, but the quality of a pencil drawing also depends on the paper used. Pencil illustrators pay as much attention to their choice of paper following the choice of pencils. Papers are made in a great variety of weights and textures. The thickness of drawing paper is determined by its weight: the heavier the paper, the thicker it is. The weight (thickness) of drawing paper w is measured in terms of grams per square meter (gsm), ranging from 48 gsm to 300 gsm . We model the paper weight as $0 \equiv thick \leq w \leq 1 \equiv thin$. Paper textures for pencil work (categorized as smooth, semi-rough and rough) have a "tooth", which is a slight roughness forming peaks and valleys that enables lead material to adhere to the paper. To represent the clusters of those peaks and valleys from real papers (see

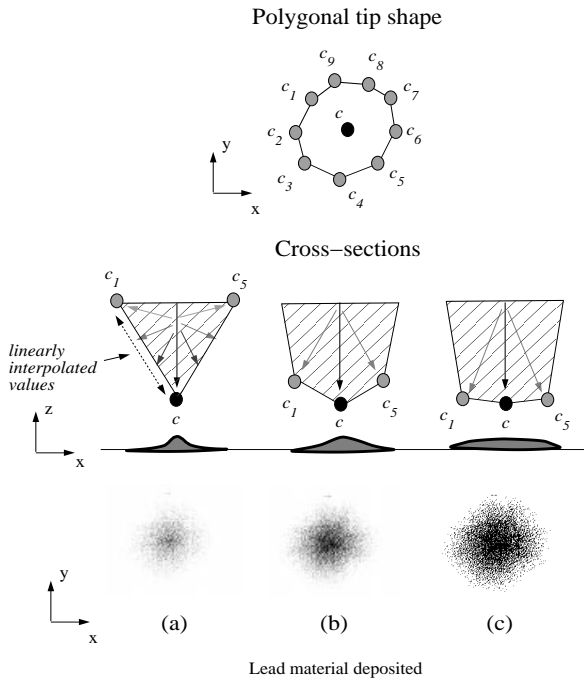


Figure 3: Different values of pressure distribution coefficients ($c, c_i, i \in [1, 9]$) across the polygonal shape result in different distribution of lead material over the paper’s surface. The results for lead material deposited are for $c = 1.0$ and the same c_i values (0.2 for (a), 0.5 for (b), and 0.9 for (c)) for all nine vertices in the polygonal tip shape.

SEM images on Figure 6) we model the paper texture as a height field $0 \leq h \leq 1$. Many of our papers are procedurally generated as reported by Curtis et al.¹³ using one of a selection of pseudo-random processes^{1, 11}. Another way of generating the paper textures is to extract the height field from the gray scale values from a digitized paper sample ($0 \equiv \text{black} \leq h \leq 1 \equiv \text{white}$). Figure 4 illustrate some of the digital samples of the papers’ surfaces used in our model. A list of variables used throughout this section is given in Table 1.

4.1. Paper Grain

The smallest element of the paper’s roughness is the grain. A grain is defined by four paper heights $h_k, k \in [1, 4]$, where h_1 is at paper location (x, y) and its three neighbors h_2 at $(x, y + dy)$, h_3 at $(x + dx, y + dy)$, and h_4 at $(x + dx, y)$ (Figure 5 (a)). The units (dx, dy) are defined in the normalized coordinate space or in the physical device coordinate space. For the results in this paper we defined each paper location (x, y) and the grain size offsets (dx, dy) equal to one pixel on a paper with total area with a resolution of 1280 x 1024 pixels. In our

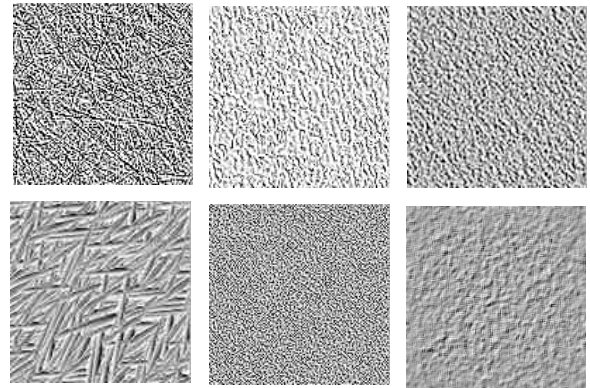


Figure 4: Examples of paper samples used in our model.

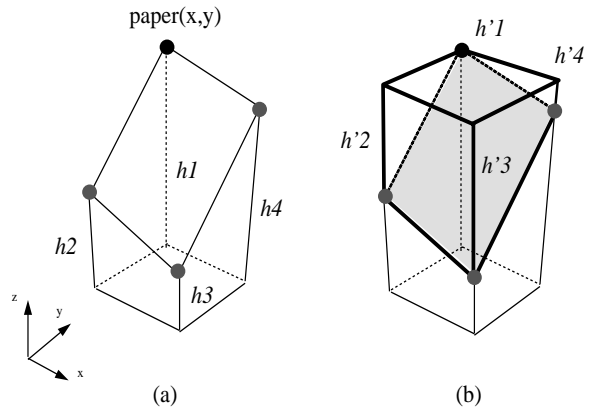


Figure 5: (a) a paper grain formed by four heights h_k with $h_{max} = h_1$, (b) the volume above the grain V_g (thicker black lines) to be filled with lead material.

model each paper location (x, y) has specific variables (indexed by k) associated with it (see Table 1).

5. Pencil and Paper Interaction

Pencil strokes are left on paper through friction between the lead and the paper. The paper grains react to the hardness of the pencil and to the pressure exerted upon it. For example, a soft pencil with a heavy pressure can make an even dark tone (Figures 1 (a), 8). The same pencil with reduced pressure makes a light tone with a grainy effect because the lead skids over the topmost fibers of the paper (leftmost sample in Figure 20). A hard pencil with firm pressure makes a light smooth tone, destroying the graininess of the paper texture (Figures 1 (b), 9).

In our system the pencil and paper interaction is modeled as follows:

for each new position of the pencil tip over the paper:

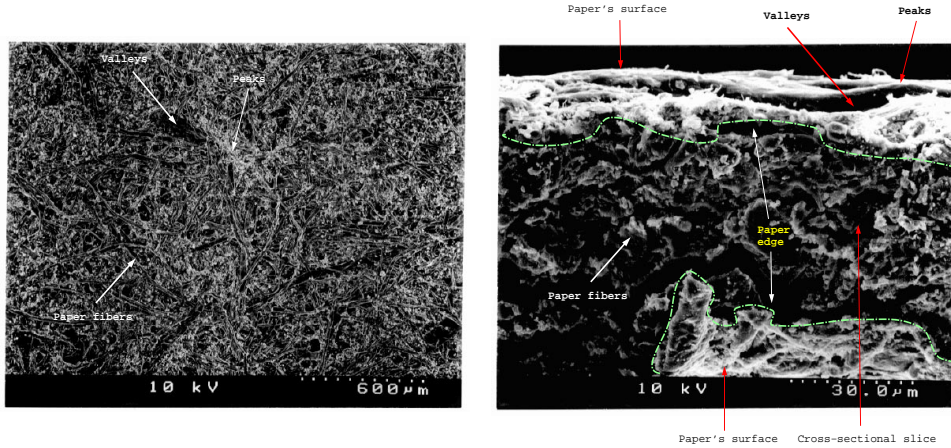


Figure 6: Aerial and cross-sectional views (left and right images respectively) from real drawing paper (medium weight, moderate tooth) generated by a scanning electron microscope (SEM) at 10 kv acceleration voltage, with different magnifications (50 times on the left image and 1000 times on the right image) and with scale resolution in microns (600 microns and 30 microns for the left and right images respectively). Paper roughness is resulting from the clustering of paper fibers forming peaks and valleys across the paper surface.

1. Evaluate the polygonal tip shape of the pencil's point (Subsection 5.1).
2. Initialize the local lead threshold volume of the paper (Subsection 5.2).
3. Distribute pressure applied to the pencil across the tip shape (Subsection 5.3).
for each paper grain interacting with the pencil tip:
 - a. Compute the grain porous threshold volume (Subsection 5.4).
 - b. Process the grain biting the lead (Subsection 5.5).
 - c. Compute damage caused by the lead to the paper grain (Subsection 5.6).

Finally, we compute the reflected intensity of lead material (Subsection 5.7).

The interaction process from each step and the illumination model evaluation are explained next. A list of variables used throughout this section is given in Table 1.

5.1. Polygonal Tip Shape Evaluation

When using pencils, different types of strokes are produced depending on the pencil's hardness, its point, and how it is applied to the paper. Also, there are many ways of handling the pencil and various effects over the stroke can be achieved^{20, 25, 24}. In our model, the canonical polygonal tip shape for any selected pencil point (Figure 2) is scaled according to the angle α defined by slanting the pencil (see Figure 7). The more the pencil is slanted, the larger the tip is. The resulting scaled tip shape resembles the general topology

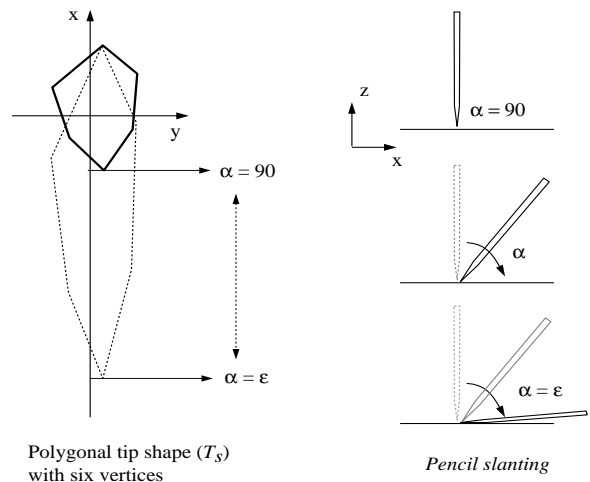


Figure 7: Scaling of the canonical tip shape of the pencil point (thicker black lines). The new shape (dotted lines) is dependent on the slanting angle α of the pencil.

of the canonical shape. A bounding box is computed for this new polygonal shape (see Figure 10). Next the point shape is rotated by β degrees based on the movements of the wrist and the whole arm (see Figure 7). Finally pressure distribution coefficients (Subsection 3.2.2, Figure 3) are assigned to the scaled polygonal shape. Variations of the tip's shape according to wear and tear along a stroke are modeled using the pencil stroke primitive¹⁸ which includes parameters that relate to the

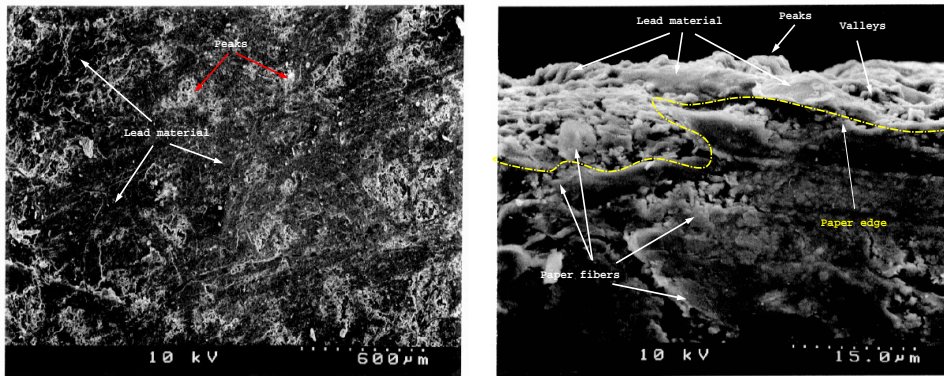


Figure 8: Aerial and cross-sectional views (left and right images respectively) from real soft-pencil drawing sample (see Figure 1 (a)) generated by a scanning electron microscope (SEM) at 10 kv acceleration voltage, with different magnifications (50 times on the left image and 2000 times on the right image) and with scale resolution in microns (600 microns and 15 microns for the left and right images respectively). On the aerial view (left image), lead material is adhered to the paper fibers filling its valleys and covering its peaks. Compare with Figure 6 (left image) and notice how the paper fibers are now barely visible because of the covering of the paper with lead material. On the cross-sectional view (right image), lead material is adhered to the paper fibers filling its valleys and covering its peaks. Compare with Figure 6 (right image) and notice how lead material (with a “cloudy” aspect) covers the paper roughness.

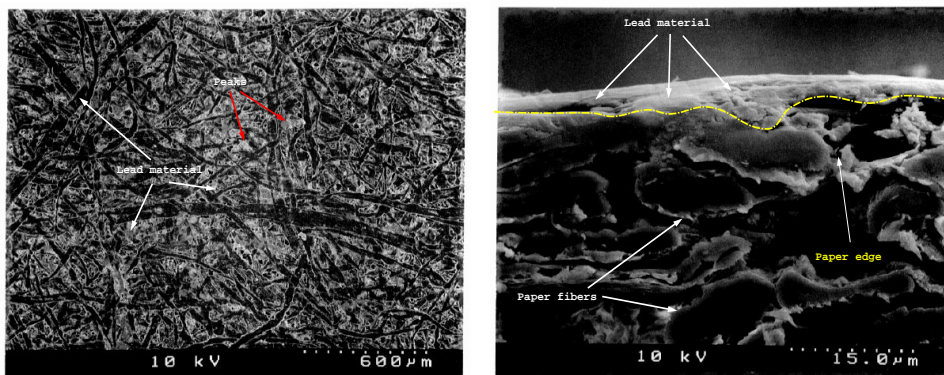


Figure 9: Aerial and cross-sectional views (left and right images respectively) from real hard-pencil drawing sample (see Figure 1(b)) generated by a scanning electron microscope (SEM) at 10 kv acceleration voltage, with different magnifications (50 times on the left image and 2000 times on the right image) and with scale resolution in microns (600 microns and 15 microns for the left and right images respectively). On the aerial view (left image), the black lines with varying thickness are the effects of the pencil point destroying the paper fibers. Compare with Figure 6 (left image) and notice the clustering of paper fibers before and after the pencil rubbing. Notice that less lead material has been deposited in comparison with Figure 8 (left image). Compare the cross-sectional view (right image) with Figure 6 and notice that the peaks and valleys from the paper grains have been totally flattened.

factors that influence a real pencil stroke (varying pressure, hand gestures, wearing and tearing of the pencil’s point).

5.2. Local Lead Threshold Volume

Each grain height h_k has a local lead threshold volume L_k , which is the maximum amount of lead material

(graphite, clay, and wax particles) that can be deposited in the grain’s height h_k (see Figure 11). The values of L_k result from the grain’s porous threshold volume computation (see Subsection 5.4). At this stage, every L_k within the bounding box of the polygonal tip shape (see Figure 10) is initialized to 0.0. This is necessary because the grain heights currently interacting with the pencil are damaged at each new pencil tip position (see Sub-

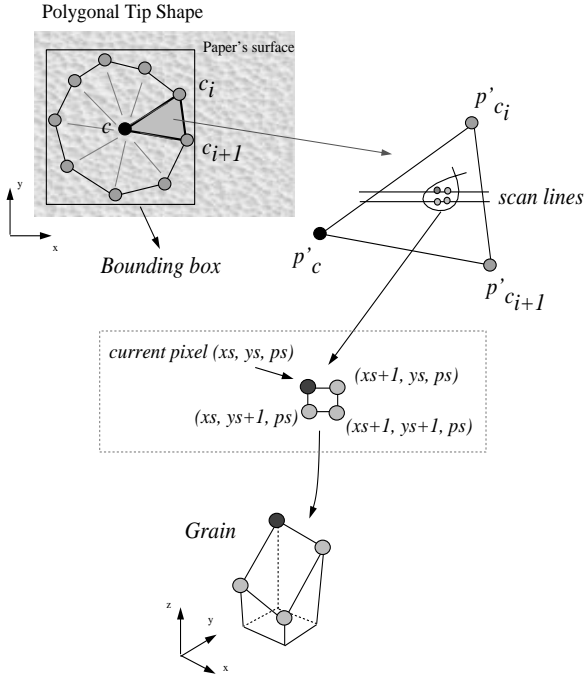


Figure 10: The pressure distribution process across the polygonal tip shape from the pencil's point.

section 5.6). This results in different L_k values at each new pencil tip position (pencil pass) on the paper.

5.3. Pressure Distribution

The pressure value applied to the pencil $p \in [0, 1]$ is distributed across the polygonal tip shape. This process considers the pressure distribution coefficients of the pencil's tip with the paper's surface (Subsection 3.2.2, Figure 3). Two steps are necessary (see Figure 10):

1. The pressure values at the pressure distribution coefficients are evaluated as:

$$\begin{aligned} p'_c &\leftarrow p \times c \\ p'_{c_i} &\leftarrow p \times c_i \end{aligned} \quad (1)$$

2. The pressure across the polygonal tip shape is computed by scan converting two lines at a time for each triangle from the polygonal tip shape, resulting in four points: the current height h at (xs, ys) and its three pixel neighbors $(xs + 1, ys)$, $(xs + 1, ys + 1)$, and $(xs, ys + 1)$, each with the correspondent interpolated pressure value ps . These four points define the paper's grain that bites the lead (see Figure 5 (a)). The four pressure values ps from the grain are averaged resulting in the pressure value P_a which will evaluate the lead interacting with the paper's grain.

5.4. Grain Porous Threshold Volume

The third processing step of the lead interacting with the paper is the computation of the lead threshold volume T_v for the grain, which is the maximum amount of lead material (graphite, clay, and wax particles) that can be deposited in the grain's volume V_g (Figure 5(b)). Two cases may occur:

1. If all the grain heights h_k are equal then T_v is equal to $F_s = 500 \text{ lpu}$ (lead particle units), which is the maximum amount of lead material necessary to fill the flat surface of the grain. Basically, only a little bit of lead gets deposited forming a thin layer.
2. If at least one of the grain heights h_k is different then the volume above the grain at (x, y) is defined by the bilinear patch whose heights are defined by

$$h'_k \leftarrow h_{max} - h_k \quad (2)$$

where h_{max} is the maximum height of the paper grain (see Figure 5). For convenience we have defined all of our grains over the unit square. Thus the volume above the grain is

$$V_g \leftarrow \frac{1}{4} \times h'_1 + \frac{1}{4} \times h'_2 + \frac{1}{4} \times h'_4 + \frac{1}{4} \times h'_3 \quad (3)$$

and T_v is given by:

$$T_v \leftarrow V_g \times F_v \quad (4)$$

where F_v is the maximum amount of lead material necessary to fill the grain's volume. Here $F_v \in [1000, 3000] \text{ lpu}$ with more lead being deposited on the side areas of the paper than on the top of flatter areas.

The values in lpu are based on our observations in which for a particular paper there is a maximum absorption rate of lead and that this can be changed according to the paper. We found that the values presented give satisfactory results for the three kinds of paper textures modeled (smooth, semi-rough, rough).

5.4.1. Lead Volume Distribution

Now we need to proportionally distribute T_v among each L_k in the grain. Each of the four k locations has a variable L_k which is the local lead threshold volume for k . We observed that the higher the height h_k is, the greater the percentage of lead material that will stick to it (see Figure 11). The distribution is computed as follows:

$$L_k \leftarrow L_k + D_k \times T_v \quad (5)$$

L_k is accumulative because it considers other neighbor grains sharing the same h_k . $D_k \in [0, 1]$ is the percentage of lead material distributed at h_k (see Figure 11):

$$D_k \leftarrow \frac{h_k}{S_h} \quad (6)$$

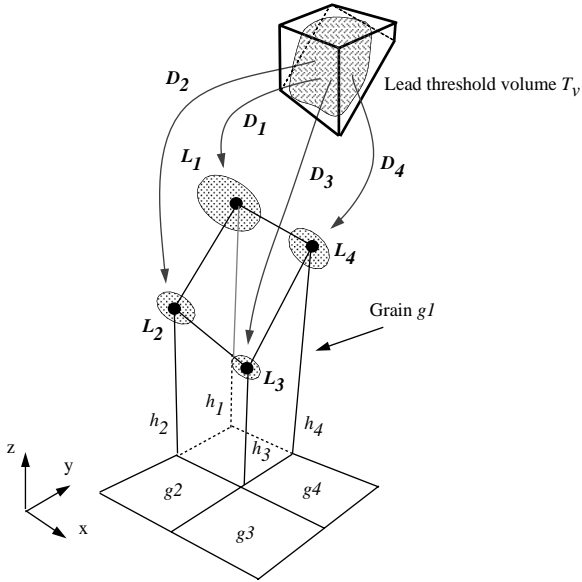


Figure 11: Proportional distribution of lead material among the grain's heights. In the example $D_1 > D_4 > D_2 > D_3$ and $D_1 + D_2 + D_3 + D_4 = 1.0$. Also h_3 is shared by the four grains g_1, g_2, g_3, g_4 . This means that h_3 accumulates lead material L_k bitten by the four grains (see Equation 5).

where $S_h \leftarrow \sum_{i=1}^4 h_i$. If $S_h = 0.0$ then $D_1 \leftarrow D_2 \leftarrow D_3 \leftarrow D_4 \leftarrow 0.25$. This means that all heights h_k from the paper grain receive the same percentage of lead material.

5.5. How Much Lead Material is “Bitten”

The amount of lead removed by the paper's grain is computed in five steps:

1. compute the depth of lead into the grain,
2. compute the volume bitten,
3. scale it according to the current lead degree,
4. distribute it among the grain's heights,
5. compute the amount of lead deposited.

Step 1: Depth of lead in the grain

The lead penetrates a certain amount into the heights h_k of the paper grain. This is computed as follows:

$$D_l \leftarrow h_{max} - (h_{max} \times P_a) \tag{7}$$

If $D_l < h_{min}$ then $D_l = h_{min}$ where h_{min} is the minimum height h_k of the paper grain. D_l will evaluate the amount of lead material bitten by the paper's grain (see Figure 12).

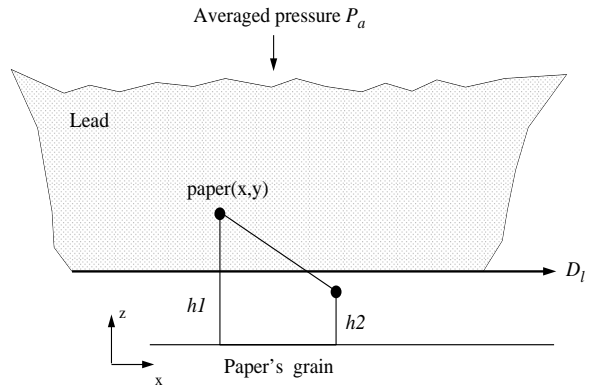


Figure 12: The heights of the paper's grain above the D_l line “bite” the lead.

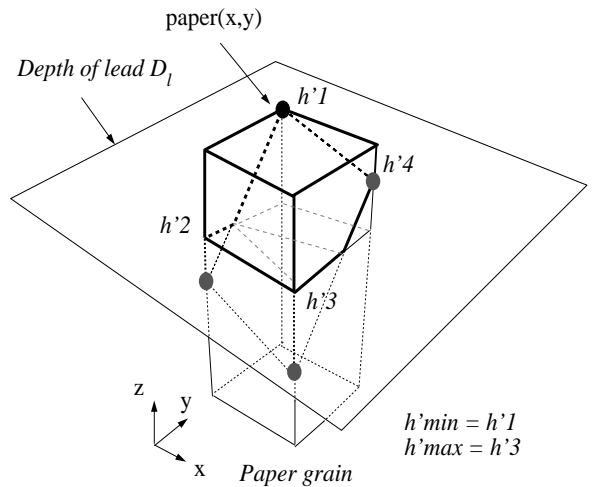


Figure 13: Refer to Figure 5(b). Grain's volume (thicker black lines) that bites the lead when the depth plane is above from at least one of the grain heights h'_k .

Step 2: Volume bitten

Lead material “bitten” by the paper's grain remains trapped among the paper's surface fibers (see Figures 6, 8, and 9).

Our model now computes the volume of lead bitten B_v by the grain. The following two cases may occur:

- a. All heights h_k are equal or above D_l meaning that the whole grain bites the lead. Here we have:

$$B_v \leftarrow T_v \tag{8}$$

- b. At least one height h_k from the grain is below D_l (see Figures 12 and 13). Here, we use a linear approximation to the volume defined by the intersection of the clipping plane defined by D_l and the bilinear surface defined by the grain's heights (Figure 13). B_v is thus

approximated by:

$$B_v \leftarrow T_v \times h_m \quad (9)$$

with

$$h_m \leftarrow \frac{(h'_{max} - D_l)}{(h'_{max} - h'_{min})} \quad (10)$$

where h'_{min} and h'_{max} are the minimum and maximum heights h'_k of the grain (Equation 2, Figures 5 (b) and 13).

Step 3: Volume adjustment

We observed that less lead is bitten from hard leads than from softer leads (see Figures 8 and 9). Hence, we need to adjust the volume of lead bitten B_v as follows:

$$B_v \leftarrow B_v \times ba(P_d) \quad (11)$$

where $ba(P_d)$ is the bite adjustment function which returns a scaling factor ($0 \leq ba \leq 1$), given the degree of the pencil being used P_d . The closer ba is to 1.0 (very soft lead), the closer the lead material is to the computed bitten volume B_v . The closer ba is to 0.0 (very hard lead), the less the bitten lead material is.

Step 4: Volume distribution

We need to proportionally distribute the grain's bitten volume B_v among the grain heights h_k . As in the lead volume distribution (Subsection 5.4.1) we observed that the higher the grain height is, the greater the percentage of lead material that will stick to it (Figure 11). This distribution is given by:

$$B_k \leftarrow B_v \times D_k \quad (12)$$

Paper grain is full

At each grain height h_k , if the total amount of lead material deposited T_k is greater or equal to the lead threshold volume L_k , then the paper grain is completely filled with lead material. Hence, it is important to progressively reduce the amount of extra lead that can be deposited. Our approach is to scale the bite volume B_k as follows:

$$B_k \leftarrow B_k \times M^p \quad (13)$$

Where p is the pressure applied to the pencil. This accounts for a decreasing ability to leave lead on a paper that is fully saturated (see Figures 1(a), 8). In our experience we have found that values $0.97 \leq M \leq 0.99$ yield realistic results.

Step 5: How much lead material is deposited

The amount of lead deposited at h_k is given by $(G_p, C_p, W_p) \times B_k$. The total amount of graphite, clay,

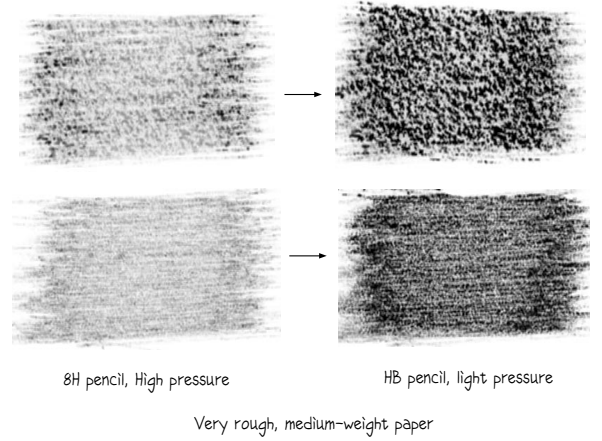


Figure 14: Our simulation model without paper damage (top row) and with paper damage (bottom row). On the top row the pencil is first applied (left) and after a while (right) notice that the amount of deposited lead material increases clearly revealing the paper grain. On the bottom row the pencil is first applied (left) and after a while (right) notice that the amount of deposited lead material increases but the paper grains are almost completely damaged.

and wax particles (G_k , C_k and W_k respectively) deposited after each pass of the pencil over the paper surface at h_k is computed as:

$$\begin{aligned} G_k &\leftarrow G_k + G_p \times B_k \\ C_k &\leftarrow C_k + C_p \times B_k \\ W_k &\leftarrow W_k + W_p \times B_k \end{aligned} \quad (14)$$

Finally, the total amount of lead material deposited at h_k is given by

$$T_k \leftarrow G_k + C_k + W_k \quad (15)$$

5.6. Paper Damage Computation

Paper grains are flattened because of the pressure P_d and hardness of the lead, which is determined by its degree P_d . We observed that harder leads damage the paper grains more than softer leads (see Figures 6, 8, and 9). For every grain's height h_k that bites the lead, the amount of paper damaged E_k is computed as follows:

$$E_k \leftarrow D_l \times da(P_d) \times w \quad (16)$$

where $da(P_d)$ (damage adjustment) is a function returning a scaling factor ($0 \leq da \leq 1$), given the pencil degree P_d used. When da is close to 1.0 there is a large amount of paper damaged which can be similar to the value of D_l . The closer da is to 0.0 (very hard lead), the more

paper is damaged. The closer da is to 0.0 (very soft lead), the less paper is damaged. The closer w is to 0.0 (very thick paper) the more resistant the paper is to the lead. This means that less paper is damaged. The grain's height h_k is then adjusted as follows:

$$h_k \leftarrow h_k - E_k \quad (17)$$

When h_k is equal to 0.0 the grain has been totally flattened. Figure 14 illustrates the effects of paper damaging using our system.

5.7. Intensity Value of Deposited Lead Material

Finally, we compute the reflected intensity of lead material I_k deposited at paper location h_k . We assume that graphite particles are black and clay and wax particles are optically neutral components. The reflected intensity depends on the amount of graphite present at h_k which is computed as follows:

$$A_k \leftarrow \frac{G_k}{F_t} \quad (18)$$

where $F_t \leftarrow F_s + F_v$ is the maximum amount of lead material necessary to cover the paper's flat surface (F_s , Subsection 5.4) and to fill the grain's volume (F_v , Subsection 5.4). The reflected intensity $I_k \in [0, 1]$ is then given by:

$$I_k \leftarrow 1.0 - A_k \quad (19)$$

6. Blender and Eraser Model

In this section we present a blender and eraser model¹⁷ that extends our graphite pencil and paper model (Sections 3, 4, 5). This blender and eraser model enhances the rendering results producing realistic looking graphite pencil tones and textures. Our model is based on observations on the absorptive and dispersal properties of blenders and erasers interacting with lead material deposited over drawing paper. The parameters of our model are the particle composition of the lead over the paper, the texture of the paper, the position and shape of the blender and eraser, and the pressure applied to them. We demonstrate the capabilities of our approach with a variety of pencil swatches and compare them to digitized pencil drawings (Figures 22, 23). We also present automatic and interactive image-based rendering results implementing traditional graphite pencil tone rendering methods (Figures 25–29). The methods in this chapter are similar to that of Sections 3, 4 and 5.

This section is organized as follows. In Subsection 6.1 we present the blender and eraser model. In Section 7 we describe in detail the modeling of the processes involved when blenders and erasers interact with lead material and paper. In Subsection 8.3 we show results from our models on different paper textures, various pencil swatches, and on tone rendering methods.

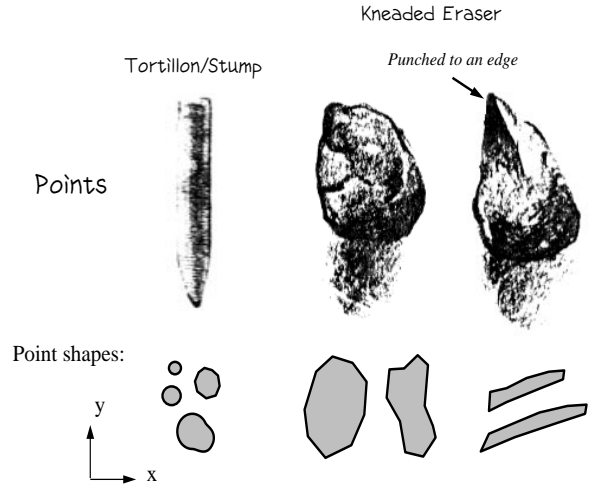


Figure 15: Different kinds of canonical points for blenders/erasers and their polygonal shapes modeling the surface area in contact with the paper.

6.1. Materials

A blender is any tool that can be used to soften edges or to make a smooth transition between tone values. We modeled two kinds of blenders:

- Tortillon, which is a cylinder, made of paper rolled into a long, tapered point at one end for blending tiny areas and fine lines.
- Stump, which is not as thin and pointy as a tortillon. Made of compressed paper, felt, or chamois, a stump can have up to a half-inch diameter.

Erasers remove surface particles to lighten a drawing. We modeled the kneaded eraser which is one of the most effective erasers made for graphite pencil. It can be used to lighten tones leaving white areas that have been covered, and it does not leave eraser dust behind. Kneaded erasers come in rectangular blocks. A piece of it is cut or torn off and kneaded between thumb and fingers until it becomes soft and pliable. It can be modeled into any shape (Figure 15).

A list of variables used throughout this section is given in Table 3.

6.1.1. Tip Shapes

The tip shapes for blenders and kneaded erasers are defined as a polygonal outline based on the shape of canonical types of points (Figure 15). This approach is similar to the modeling of pencil points (Subsection 3.2.1). A blender/eraser tip is defined as $T_s = \{(x_i, y_i), s : 3 \leq i \leq n\}$, where (x_i, y_i) is one the n vertices of the polygon and s is the scale factor of the polygon used to account for the width of the blender/eraser.

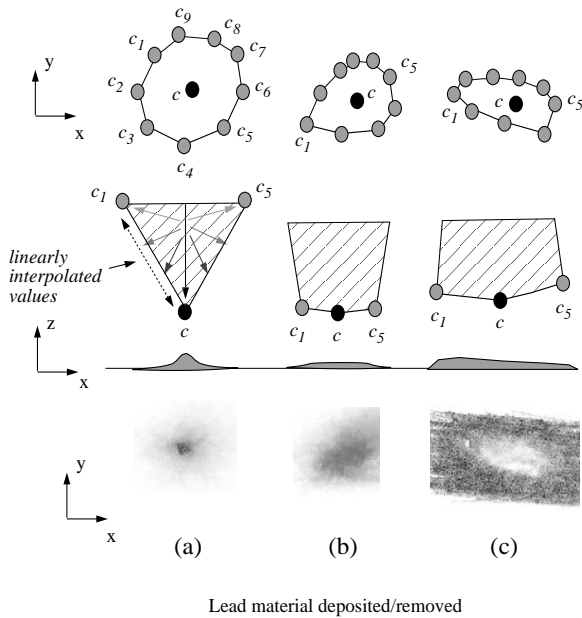


Figure 16: Examples of the xy polygonal shape, cross-sectional views, and results using our model for (a) tortillon and (b) stump blenders, and (c) kneaded eraser. Different values of pressure distribution coefficients (c and c_i) across the polygonal shape result in different deposit and removal of lead material over the paper's surface. The results for lead material blended are for $c = 1.0$ and the same c_i value for all vertices in the polygonal shape ((a) 0.2 for the tortillon, (b) 0.5 for the stump). The result for lead material erased (c) has $c = 1.0$ and c_i values with slight variations between 0.7 and 0.9.

6.1.2. Pressure Distribution Coefficients

Pressure distribution coefficients are values between 0 and 1 representing the percentage of the blender's and eraser's point surface that, on average, makes contact with the paper. This value will locally scale the pressure being applied to the blender/eraser. The pressure distribution coefficients are defined as $P_c = (c, x, y), (c_i, x_i, y_i) : 1 \leq i \leq n$ where c is the value of the main pressure distribution coefficient whose location (x, y) can be anywhere within the polygon defining the tip shape (default location is at the center of the polygon), and c_i is the value of the pressure distribution coefficient at vertex (x_i, y_i) from the polygonal tip shape. Different values can be assigned to c and to each c_i . The closer they are to 1.0, the more surface is in contact with the paper. The closer they are to 0.0, the less surface is in contact with the paper. The values between c and c_i are computed by linear interpolation, thus defining the general shape of the blender/eraser tip (see Figure 16).

7. Blender and Erasers Interacting with Lead and Paper

By flattening out a kneaded eraser, placing it firmly over an area, and then pulling quickly, lead material will be lifted away without rubbing the paper surface. As the kneaded eraser rubs the paper's surface lead material is removed sticking completely to the eraser's point. No lead material is deposited back on the paper (Figures 16(c), 17).

We modeled this interaction process in three main steps:

- Evaluate the polygonal shape of the eraser's point (Subsections 5.1 and 7.2).
- Distribute pressure applied to the eraser across its point (Subsection 5.3).
- Process the removal of lead material (Subsection 7.4).

Blending changes the texture of an image. When a graphite pencil is drawn across a surface, it leaves particles on top of the paper fibers. The empty valleys lead to a textured look to a line or an area of tone. Blending pushes the lead into the surface so that the paper's low grains become filled. This results in tones that seem smoother, more intense, and deeper in value. As the blender rubs the paper's surface, lead material is removed sticking to the blender's point, and a certain amount of lead material is then deposited back on the paper (Figures 16(a, b), 18). The third step for blenders involves both the removal and the deposit of lead material.

The interaction process for each step for blenders and kneaded erasers is explained next.

7.1. Polygonal Shape Evaluation

The canonical polygonal shape for any selected blender's and eraser's point (Figure 15) is scaled according to the pressure applied over it. Next the point shape is rotated by β degrees based on the movements of the wrist and the whole arm. A bounding box is computed for this new polygonal shape. Finally pressure distribution coefficients (Subsection 6.1.2) are assigned to the scaled polygonal shape.

7.2. Blender Buffer

Every blender has a buffer associated with it. This buffer keeps track of the current amount of lead material deposited and removed because of interaction with the paper (Subsection 7.4). Kneaded erasers do not need this buffer because they only remove lead. The buffer is an array of pixels with the same resolution from the bounding box of the current evaluated polygonal shape defining the blender (Figure 19). At each location (x_b, y_b) on the buffer we store and remove lead material

Blender and Eraser model	
T_s	Tip shape (Subsection 6.1.1, Figure 15).
P_c	Pressure distribution coefficients (Subsection 6.1.2, Figure 16).
Blender/Eraser interaction with lead and paper	
p	Pressure applied to the blender/eraser (Subsection 7.3, Figure 19).
p'_c, p'_{c_i}	Blender/eraser pressure at the pressure distribution coefficients P_c (Subsection 7.3, Equation 20, Figure 19).
(x_s, y_s, p_s)	Interpolated coordinates and pressure at the tip shape T_s (Subsection 7.3, Figure 19).
lmr	Amount of lead removed from paper (Subsection 7.4, Equations 21, 24).
$lm_{(x,y)}$	Lead material deposited on paper(x,y) (Subsection 7.4, Equations 22, 26, Figure 19).
$lm_{(x_b,y_b)}$	Lead material deposited on the blender buffer (x _b ,y _b) (Subsection 7.4, Equations 23, 25, Figure 19).
t	Absorption/storage capacity of lead material in the blender (Subsection 7.4, Equations 25, 26).

Table 3: List of variables used for the blender and eraser model.

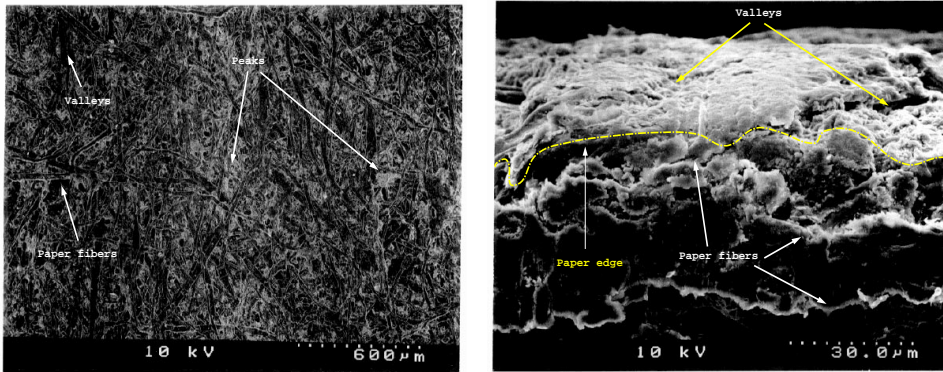


Figure 17: Aerial and cross-sectional views (left and right images respectively) from real kneaded eraser sample (see Figure 1 (d)) generated by a scanning electron microscope (SEM) at 10 kv acceleration voltage, with different magnifications (50 times on the left image and 1000 times on the right image) and with scale resolution in microns (600 microns and 30 microns for the left and right images respectively). On the aerial view (left image), compare with Figures 6 and 8 and notice the reduction of lead material from the paper. Observe that paper fibers are also more visible, revealing a similar roughness structure to the paper in Figure 6. Black lines with varying thickness are because of paper fibers damaged by the eraser. On the cross-sectional view (right image), compare with Figures 6 and 8 and notice how lead material has been progressively removed revealing a similar structure to the original paper roughness in Figure 6.

$lm_{(x_b,y_b)}$. For the first polygonal shape every buffer location (x_b, y_b) is initialized to 0. If the polygonal shape changes then only the size of the buffer is adjusted, preserving the information about lead material that has already been deposited and removed.

7.3. Pressure Distribution

The pressure value applied to the blender/eraser p ($0 \leq p \leq 1$) is distributed across the polygonal shape defining the blender's and eraser's point. This process considers the pressure distribution coefficients of the blender's and eraser's point with the paper's surface (Subsection 6.1.2). Two steps are necessary (Figure 19):

- The pressure values p' at the pressure distribution coefficients are evaluated as:

$$\begin{aligned} p'_c &\leftarrow p \times c \\ p'_{c_i} &\leftarrow p \times c_i \end{aligned} \quad (20)$$

- The pressure across the polygonal shape is computed by scan converting one line at a time for each triangle from the polygonal shape, resulting in the location (x_s, y_s) with the correspondent pressure value p_s .

We have found that the values for $plr(0.7,0.5)$ and $t(0.2,0.5)$ give credible results. They are based on our observations on the absorption and dispersion behavior of blenders and erasers over deposited lead material.

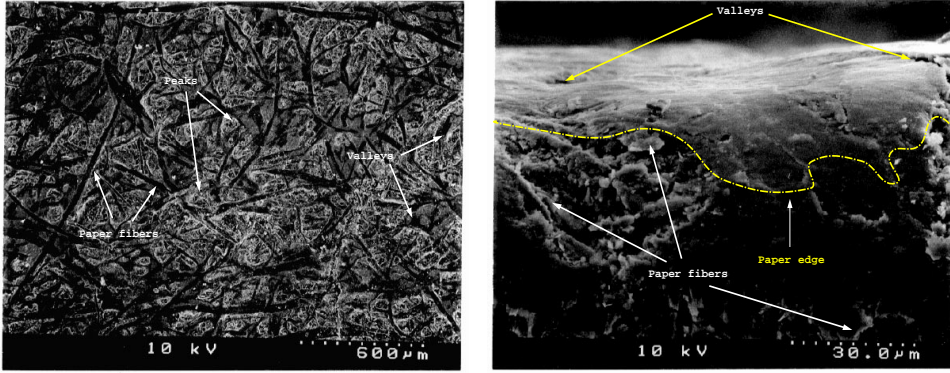


Figure 18: Aerial and cross-sectional views (left and right images respectively) from real blender sample (see Figure 1(c)) generated by a scanning electron microscope (SEM) at 10kv acceleration voltage, with different magnifications (50 times on the left image and 1000 times on the right image) and with scale resolution in microns (600 microns and 30 microns for the left and right images respectively). On the aerial view (left image), the blending process creates large areas with a uniform distribution of lead material deposited on them. These areas have similar shapes and are regularly distributed across the paper surface. Compare with Figures 6 and 8 to better visualize the before and after effects of blending. Black lines are paper fibers damaged by the blender. On the cross-sectional view (right image), compare with Figure 8 and notice how lead material has been uniformly distributed across the paper surface, covering its peaks and valleys.

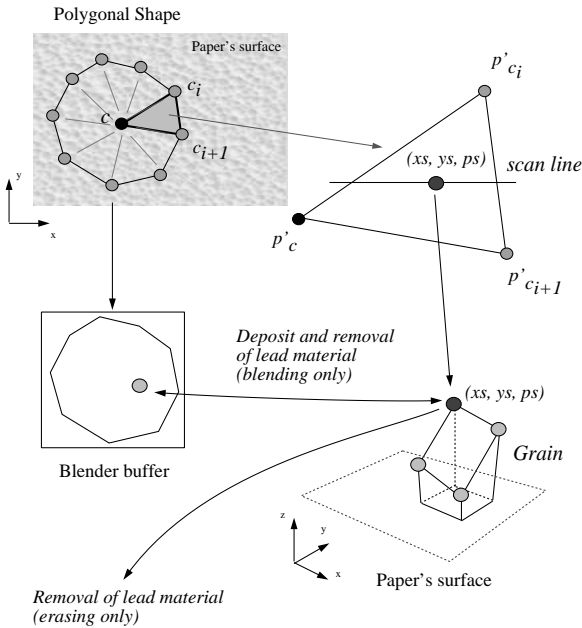


Figure 19: The pressure distribution process across the polygonal shape from the blender's and eraser's point.

For a kneaded eraser only steps 1 and 2 from *paper to blender* are necessary.

7.4. Deposit and Removal of Lead Material

The transfer of lead material from paper to blender and from blender to paper is computed as follows:

From paper to blender

- a. A certain amount of lead material lmr is removed from paper (x, y) :

$$lmr \leftarrow lm_{(xs,ys)} \times (ps \times plr), plr = 0.7, \quad (21)$$

where plr is the percentage of lead material removed.

- b. The amount of lead material on the paper is reduced:

$$lm_{(xs,ys)} \leftarrow lm_{(xs,ys)} - lmr \quad (22)$$

- c. Lead material lmr removed from the paper is deposited on the blender buffer (xb, yb) :

$$lm_{(xb,yb)} \leftarrow lm_{(xb,yb)} + lmr \quad (23)$$

From blender to paper

- a. A certain amount of lead material is removed from blender (xb, yb) :

$$lmr \leftarrow lm_{(xb,yb)} \times (ps \times plr), plr = 0.5 \quad (24)$$

- b. The amount of lead material on the blender is reduced:

$$lm_{(xb,yb)} \leftarrow lm_{(xb,yb)} - (lmr \times t) \quad (25)$$

where t ($0 \leq t \leq 1$) models the absorption/storage capacity of lead material in the blender. The closer t is to 0 the greater the absorption/storage capacity of the blender. We defined $t = 0.2$ for tortillons and $t = 0.5$ for stumps.

- c. Lead material lmr is deposited on the paper (xs, ys) :

$$lm_{(xs,ys)} \leftarrow lm_{(xs,ys)} + (lmr \times t) \quad (26)$$

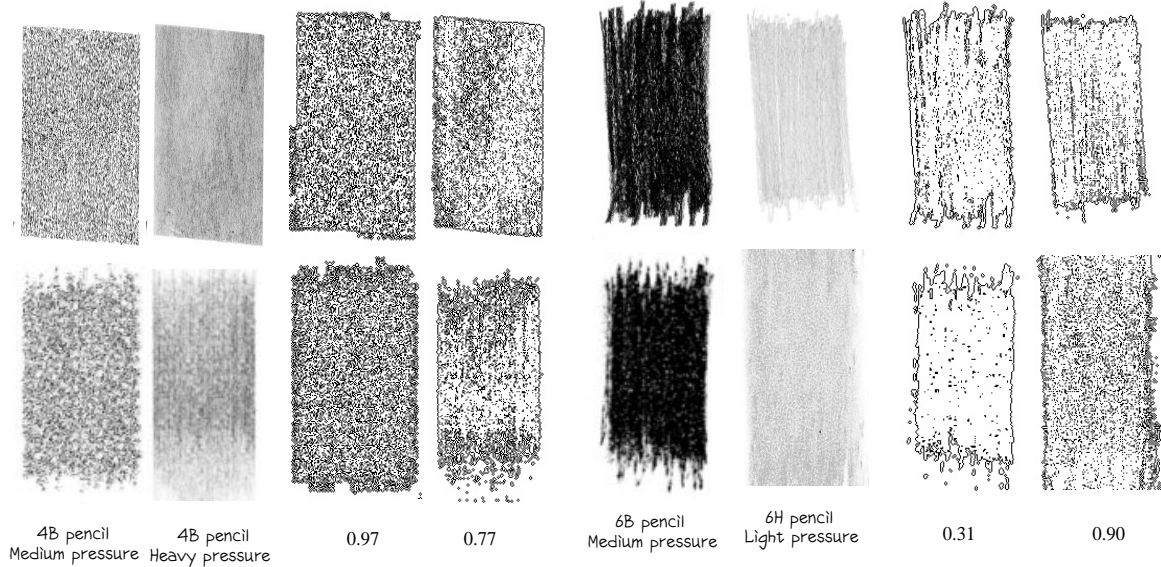


Figure 20: Our simulation model applied over drawing paper (bottom row). Compare results with real pencil work (top row). Notice that our simulation results have a good approximation to the gray level intensity because of a well-distributed amount of lead material across the paper's surface. The damage to the paper grain is also satisfactory as the perceived roughness of the paper's surface from both the real and simulated models is approximately the same. Contour maps are also presented for the results. Values represent the threshold median intensity value. The top row is from real pencil and bottom row from our pencil and paper model. This is an alternative way of visualizing the distribution of lead material across the paper's surface. The evaluation criterion is that the distribution of contour lines from the real samples should be approximately the same as the simulated samples. Based on this criterion our model makes a satisfactory distribution of lead material across the drawing.

8. Results

All the results were generated on an SGI OCTANETM Power Desktop[‡] and printed at 200 *dpi* on a 600 *dpi* HP LaserJet 5Si MX printer. Real samples were scanned at 150 *dpi*. We adapted our models (pencil and paper, blender and eraser) to an interactive illustration system using procedural and digital samples for the paper's texture. The response time was satisfactory at interactive rates. The computational cost is due mainly to the evaluation of the interaction among the models (Sections 5, 7) at each pixel (approximately 2E-5 seconds).

8.1. Evaluation

To evaluate the models we chose representative swatches of real pencil drawings and used our system to duplicate the effect. Our evaluation is thus conducted by observing how close to the original swatches are the computer-generated ones. The images from the results show that our simulation models qualitatively capture

many effects observed in real pencil work. In addition, contour maps were generated for both the real and simulated sample results for every intensity value less than or equal to the median intensity value. The evaluation criterion is that the distribution of contour lines from the real samples should be *approximately* the same as the simulated samples. Based on this criterion our model makes a satisfactory distribution of lead material across the drawing paper (see Figures 20, 21, 22, 23).

8.2. Pencil and Paper Model

Paper damage

Figure 14 illustrates the effects of paper damage after rubbing pencils over it. A canonical broad pencil shape is used. Our approach was to rub a hard pencil and then a softer one to reveal the paper grains. The upper row of Figure 14 illustrates no damage to the paper and the bottom row illustrates damage to the paper.

Individual tones

The bottom row of Figure 20 illustrates results from our model by using different textures of drawing papers and

[‡] All rendering is done in software.

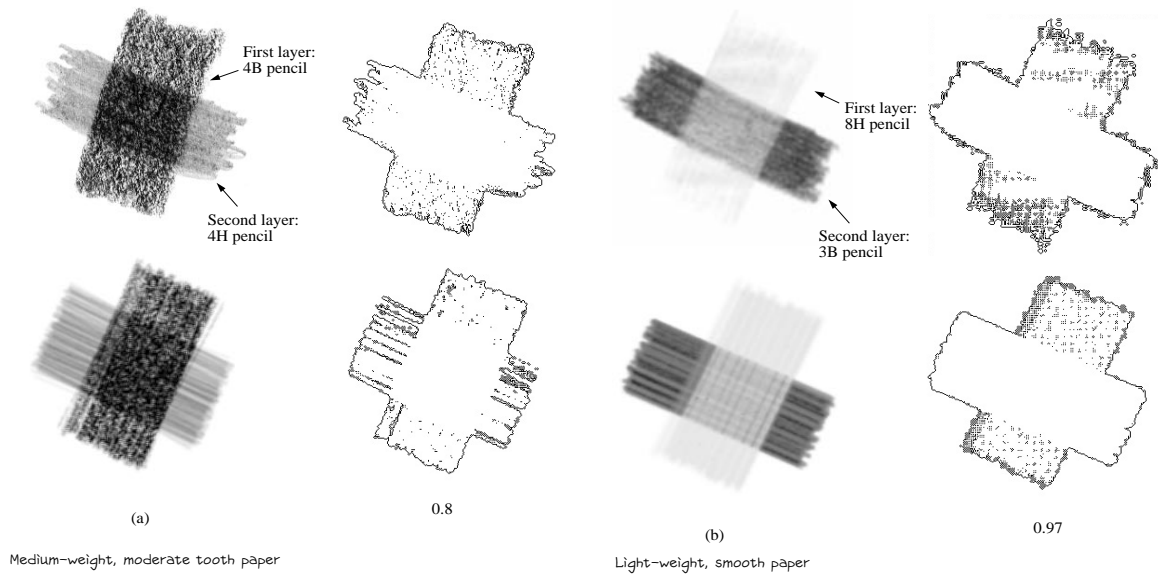


Figure 21: Real (top row) and simulated (bottom row) examples of pencil swatches illustrating the blending effects from layering lead material over drawing paper. Note that our simulation results have a good approximation to the gray level intensity because of the blending of lead material from different pencil grades (intersection area of the two layers of swatches). Pencils were slanted by $\alpha = 45.0$ degrees, sharpened with a broad point. Simulated results were generated automatically by the mark-making primitive¹⁸ taking about 30 sec. for each layer of lead material. (1) first layer: light pressure, rubbing a few times; second layer: light pressure, rubbing a few times with pencil a little bit slanted. (2) first layer: light pressure, rubbing a few times, pencil a bit slanted; second layer: light pressure, rubbing a few times. Contour maps are also presented for the results. Values represent the threshold median intensity value. The top row is from real pencil and bottom row from our pencil and paper model. Note that the distribution of contour lines in the intersection area of the two layers of swatches is equal for both the real and simulated results. This means that our model has a good approximation of the distribution and blending of lead material from two different pencil grades.

testing the effects of lead material over them, including paper damage (see Figure 14). In addition, we present in the same figure scans of real pencil work to compare with results from our model. The paper texture of Figure 20 with 4B pencil applied was computed from a digitized sample. The paper texture of Figure 20 with 6B and 6H pencils applied was procedurally generated.

Layers of tones

It is important to illustrate the effects of layers of soft lead material over layers of hard lead material, and vice-versa. In this manner, we build areas of tones that are used to describe forms and light. In Figure 21(a) a soft pencil is first rubbed over the paper in one direction and then rubbing a hard pencil over the top at an angle to the first. The result is that the intersection area between the two layers of lead material gets darker. In Figure 21 (b) we do the opposite, a layer of a soft lead on top of a layer of a hard lead. This illustrates how full grains can be slightly altered by successive passes, but the effect is minimal. Compare results from our model

with scans of real pencil swatches presented in the top row of Figure 21.

8.3. Blender and Eraser Model

Individual tones

This first set of results illustrates the effects of blending (Figure 22) and erasing (Figure 23) pencil swatches over medium-weight, semi-rough paper's surfaces. To evaluate the blender and eraser model we chose representative swatches of real pencil drawings and used our system to duplicate the effect. Besides this we used a thresholded contour display that gave us some further insights into the distribution of the graphite. This is the same approach used for the first set of results for the pencil and paper model (Subsection 8.1, Figures 20, 21). The images from the results show that our simulation model produces similar results to the strokes and swatches generated with real blenders and kneaded eraser over lead material on drawing papers. This means that our model makes a satisfactory dispersion and absorption of lead

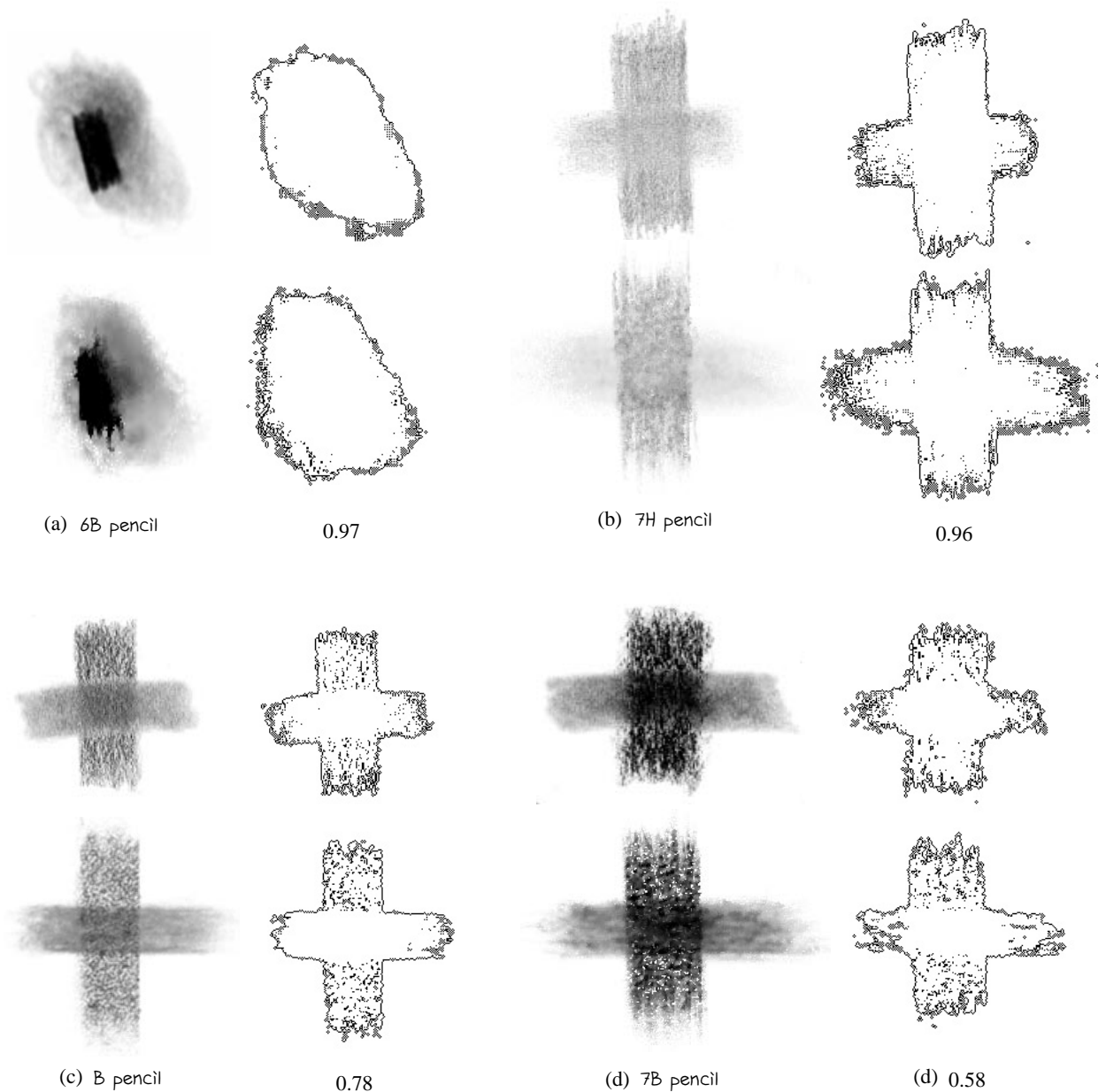


Figure 22: The bottom row shows results from our blender model applied over the pencil and paper model. Compare results in the blended area with real pencil work (top row). For blenders: (a) a 6B pencil was rubbed firmly and then a tortillon was rubbed over it with circular gestures and medium to low pressure (20 sec.); (b), (c), and (d): pencil strokes were rubbed vertically and then stumps were rubbed horizontally (15–25 sec.). Contour maps are also presented for the results. Values represent the threshold median intensity value. Note that the distribution of contour lines is approximately the same between the real and simulated results. This means that our model has a good approximation of the distribution of lead material after the blending process.

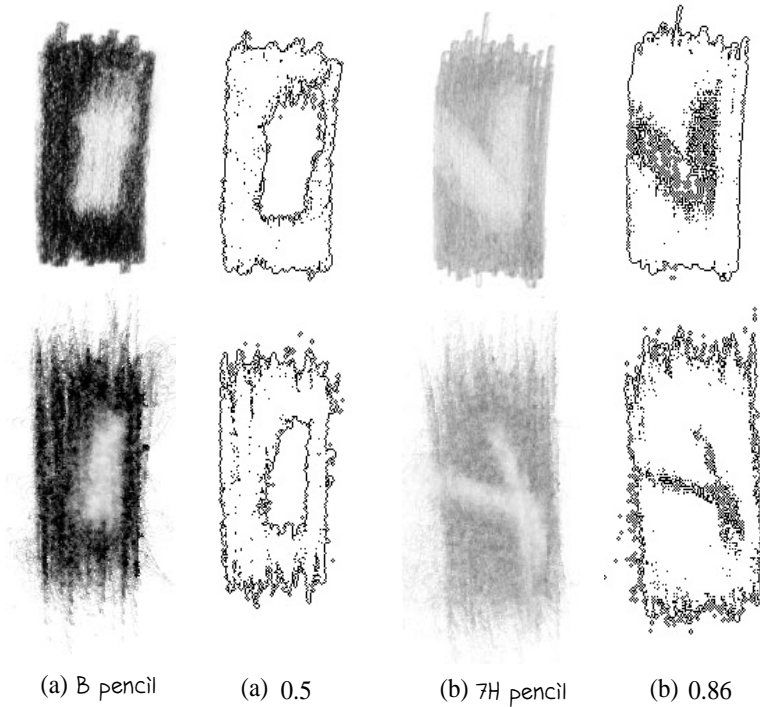


Figure 23: The bottom row (a), (b) shows results from our kneaded eraser model applied over the pencil and paper model. Compare results in the erased area with real pencil work (top row); (c) (d) illustrate the contour maps for (a), (b) respectively, with values representing the threshold median intensity. Note that the distribution of contour lines is approximately the same between the real and simulated results. This means that our model has a good approximation of the absorption of lead material after the erasing process.

material across the drawing paper (see Figures 22 and 23).

Tone rendering using smudge

The second set of results illustrates results for tone rendering using a method called smudging. The images were generated using methods for blenders and kneaded erasers recommended by review of pencil literature and contact with artists and illustrators^{21, 22, 23, 25}. Blenders and kneaded eraser are excellent for this rendering method, used for illustrating soft subject matter and shadows. Three rendering stages are necessary:

- The tone values in the subject are rendered by using one pencil hardness (degree).
- Certain portions of the drawing are smudged using blenders.
- A kneaded eraser is then used to lighten the areas where there are highlights.

Figure 24 illustrates a real pencil work using blenders and kneaded erasers.

We demonstrate several image-based rendering results for smudging using the models presented. We use reference images of one real pencil drawing (Figure 25, (*sphere*)), four real pen-and-ink illustrations (Figures 25, (*cup*), 26, 27, and 28), and one photograph (Figure 29). The intensity values i at each pixel (x, y) on the reference images define the height field h of the paper's surface where $h_{(x,y)} = i_{(x,y)}$. Our goal was to create a pencil rendered version for each of the reference images. The rendering pipeline consists of two stages:

First rendering stage

This first stage is done automatically by our system (part (b) from Figures 25 to 29) by scan-converting the reference image (paper texture). For each paper location (x, y) (correspondent to the reference image pixel location (x, y) in the scan line) the pencil and paper model is evaluated (Section 5).

The computational cost of this stage is due mainly to the evaluation of the pencil point from the pencil and paper model at each pixel on the reference image. The total cost = Number of pixels on the image \times Pencil

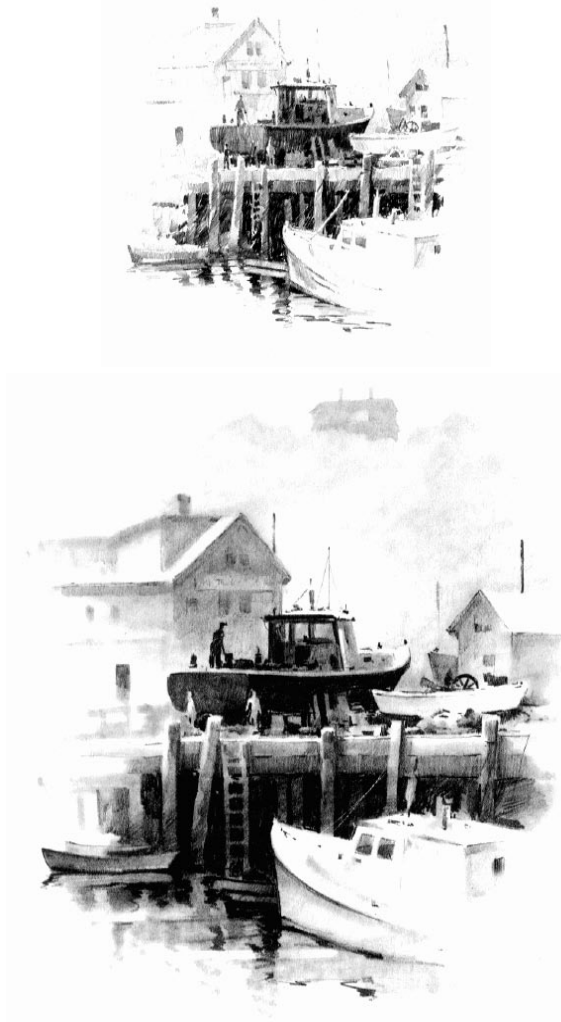


Figure 24: Example of real pencil work using the smudging effects²². The drawing in the top row was done with pencils alone. The drawing in the bottom row was smudged.

and paper interaction process evaluated at each pixel on the polygonal shape for the pencil point. For the results in this paper we use a pencil point with size equal to one pixel to match the scanline process. The response time was satisfactory at interactive rates (see figures' captions).

For each pixel at paper (x, y) from the scan line, the intensity $i_{(x,y)}$ will adjust the pressure p applied to a single pencil resulting in the correct amount of lead material deposited at paper (x, y) . The pressure p applied to the pencil is the only parameter that changes at this stage, and it is given by $p = 1.0 - i_{(x,y)}$. This means that

to achieve a darker intensity more pressure is required. This approach is based on traditional pencil rendering methods to create tone values²².

If the user provides additional pressure pa then the final pressure value p is scaled as $p = p \times pa$. This is the case for Figure 29 (b) where pencil strokes using our model were interactively defined over the photograph after the automatic evaluation of the pencil and paper model (Figure 29(a)) during the scan-conversion of the reference image (paper texture). Here the only parameter changed was the pressure applied to the pencil.

Second rendering stage

For this stage we adapt the blender and eraser model to an interactive illustration system. The user interactively controls the blenders and the kneaded eraser to compose the final image (part (c) from Figures 25, 26, 28, 29, and parts (c, d, e) from Figure 27). The response time was satisfactory at interactive rates (see figures' captions). For each paper location (x, y) (correspondent to the reference image pixel location (x, y)) the blender and eraser model is evaluated, with c (main pressure distribution coefficient, Subsection 6.1.2, Figures 16, 19) from the blender's and eraser's point at (x, y) . The pressure distribution coefficients (c and c_i) have values equal to 1.0. For the results in this chapter we use blender and eraser polygonal shapes with resolutions of 1–10 pixels. Like in the first stage, the pressure p applied to blenders/erasers is also adjusted according to $i_{(x,y)}$. Here $pi_{(x,y)} = i_{(x,y)}$, this means that to achieve a lighter intensity more pressure is required.

9. Conclusions and Future Work

In this paper we presented results from our research in pencil illustration methods for non-photorealistic rendering. The main motivation for this work is to investigate graphite pencil as a useful technical and artistic NPR production technique to provide alternative display models for users. Our approach is based on an observational model of the interaction among real graphite pencil drawing materials (pencil, paper, eraser, blender). The goal was to capture the essential physical properties and behaviors observed to produce quality pencil marks at interactive rates. The images from the results show that our simulation model produces similar results to the strokes and swatches generated with real graphite pencil materials. To evaluate the system we chose representative swatches of real pencil drawings and used our system to duplicate the effect. Our evaluation is thus conducted by observing how close to the original swatches are the computer-generated ones. Besides this we used a thresholded contour display that gave us some further insights into the distribution of lead material on paper. The models in this paper can be

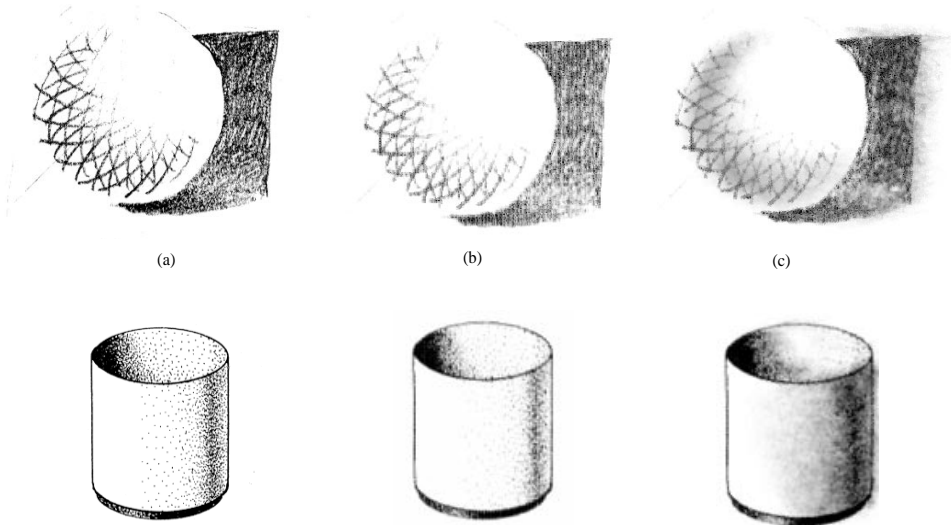


Figure 25: (a) Real pencil drawing of a sphere (resolution of 283×218 pixels) rendered using a very soft pencil and cross-hatching to convey tone values (top row); a cup rendered in pen-and-ink (resolution of 240×282 pixels) using ink dots (bottom row). Next stages using our simulation models: (b) Automatic rendering using 2B pencil (1.24 sec. for the sphere and 1.36 sec. for the cup). (c) Smudging the crosshatched lines on the sphere (30 sec.) and the ink dots on the cup (25 sec.) creating a better effect on the tone. Shadow is also smudged around the sphere to make it softer. Notice the excess of graphite, which spreads as we smudge the drawing. Kneaded eraser enhances highlight and clears some portions of the shadows (8 sec. for the sphere and 10 sec. for the cup)

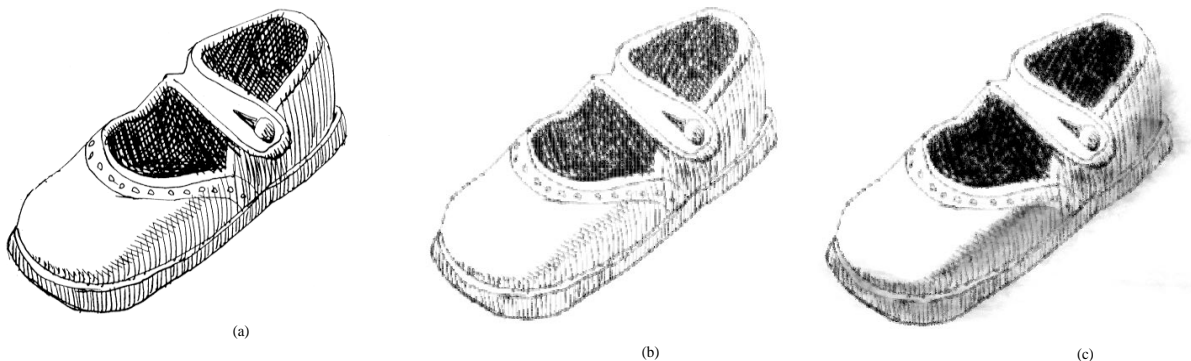


Figure 26: (a) Real pen-and-ink illustration of a shoe (resolution of 402×345 pixels) rendered using a few simple tones that created the illusion of form and depth. (b) Automatic rendering using 3B pencil (2.79 sec.). (c) Smudging the lines (30 sec.) and then applying the kneaded eraser on top and inside the shoe enhancing its tonal contrast (12 sec.).

adapted to existing interactive illustration systems^{2, 5, 6} and 3D NPR systems for technical illustration, art, and design^{3, 7, 8, 9, 10, 12, 15, 16}.

The graphite pencil combines perfectly with many media, frequently playing an important part in conjunction with pen-and-ink, brush and ink, wash, watercolor, etc. We are currently investigating the extension and

the combination of our pencil model with other simulated media such as watercolor^{4, 13} and pen-and-ink^{6, 7}. We are also investigating the modeling of higher-level pencil rendering primitives built on top of the models for pencil drawing materials. These primitives can be used to extend the capabilities of existing 3D modelers/renderers to automatically render models with a look that emulates real pencil renderings¹⁸.

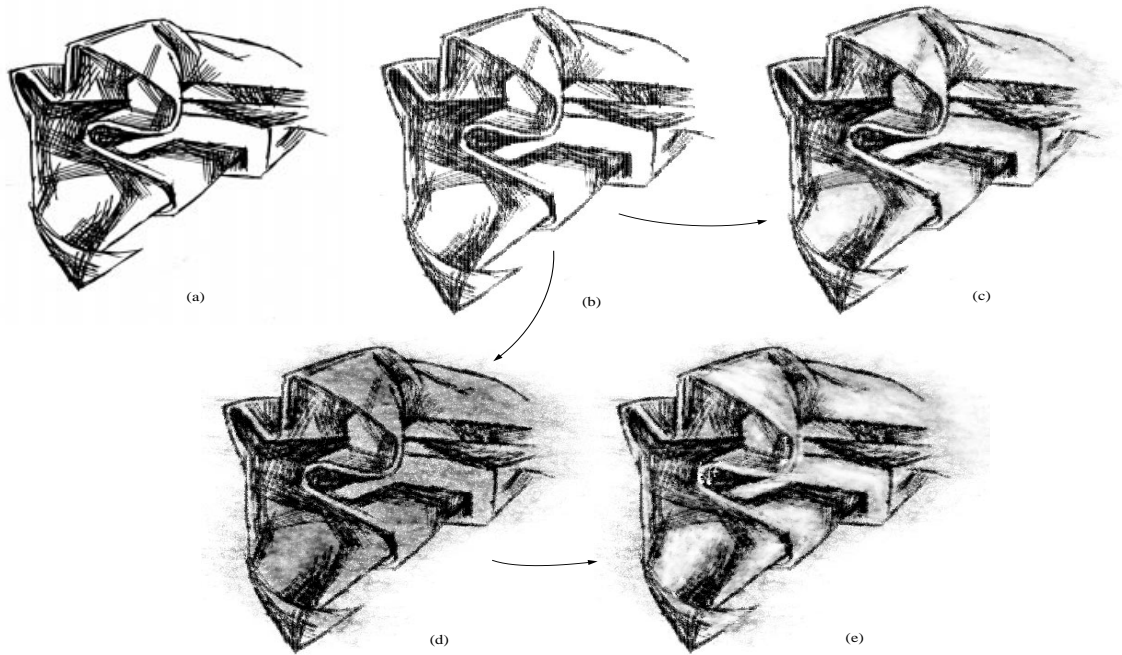


Figure 27: (a) Real pen-and-ink illustration of fabric (resolution of 323×382 pixels) accentuating folds by drawing them crisply. (b) Automatic rendering using 4B pencil (2.48 sec.). (c) Smudging and erasing certain parts (40 sec.). (d) Smudging the entire drawing from (b) in a relatively flat-tone (30 sec.) and then (e) using the kneaded eraser to set up areas of highlights (25 sec.)^{23, 19}.

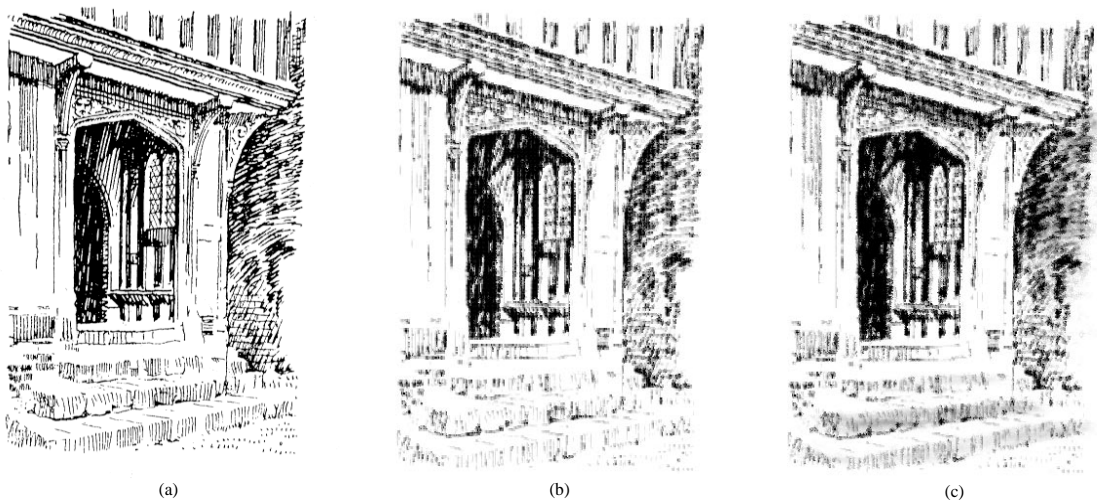


Figure 28: (a) Real pen-and-ink rendering on tracing paper (resolution of 320×408 pixels). (b) Automatic rendering using 6B pencil (2.63 sec.). (c) Smudging most of the shadow lines and the tone strokes for the bushes (35 sec.).

Acknowledgments

This research work was sponsored by the Brazilian Council of Scientific and Technological Development (CNPq) and by the Natural Sciences and Engineer-

ing Council of Canada (NSERC). The authors thank Mark Green, Ben Watson, Oleg Veryovka, Paul Ferry, and other members of the Computer Graphics Research Lab, University of Alberta for their reviews and comments. Further thanks are owed to Thomas Strothotte

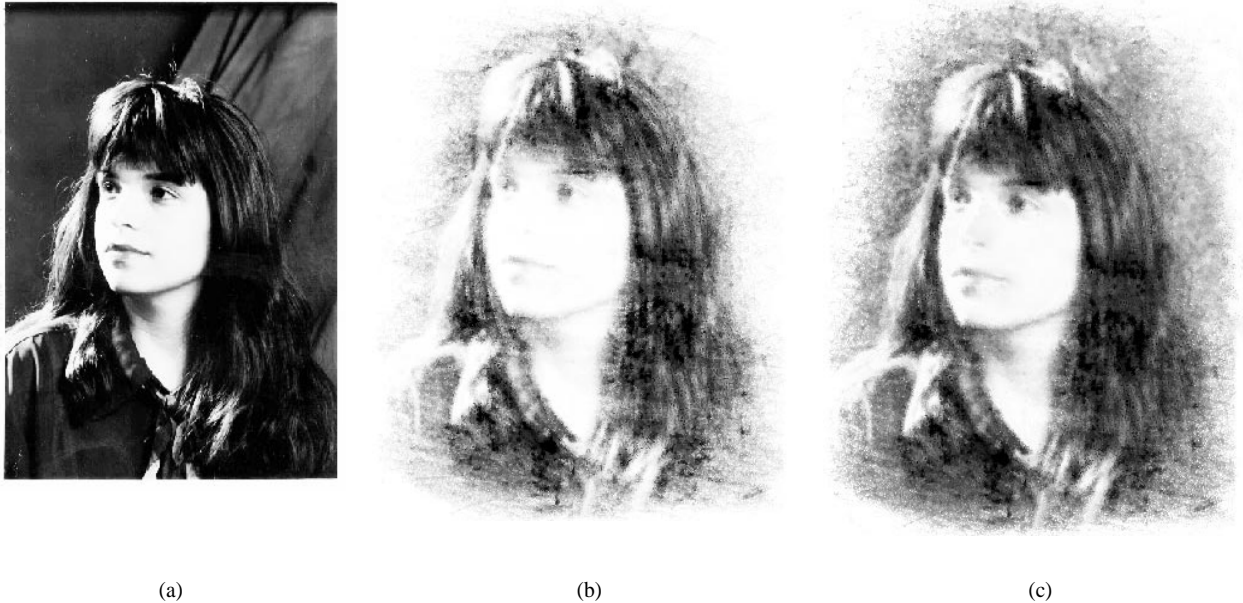


Figure 29: (a) High contrast photograph of Patricia (resolution of 279×388 pixels). (b) Automatic rendering using 6H pencil (2.18 sec.) (first stage, Subsection 4.4.2) followed by interactive rendering (pencil point from the pencil and paper model adapted to an interactive illustration system) with strokes interactively applied using medium-soft pencils applied with light pressure (15 sec.). (c) Smudging the darker tones, the background plane of the photograph, and lightly smudging the shadows and some of the face lines (40 sec.). Kneaded eraser lightly applied to emphasize the highlights (30 sec.).

of the Department of Simulation and Graphics, University of Magdeburg, Germany, and to Desmond Rochfort and Barbara Maywood of the Department of Art and Design, University of Alberta for their constructive criticism and positive comments. The authors would like to thank from the Department of Chemical and Materials Engineering, Zhenghe Xu for his insights and comments on the simulation models and Tina Barker for generating the SEM images. Our thanks also go to David Clyburn for his valuable text review, and to Paul Lalonde for his comments. The authors also thank Patricia Rebolo Medici for her reviews, comments, and photograph.

References

1. K. Perlin. An image synthesizer. *Proc. of SIGGRAPH '85*, 287–296, July 1985.
2. A.H. Vermeulen and P.P. Tanner. PencilSketch – a pencil-based paint system. *Proc. of Graphics Interface '89*, 138–143, June 1989.
3. D. Dooley and M.F. Cohen. Automatic illustration of 3D geometric models: surfaces. *Proc. of IEEE Visualization '90*, 307–314, October 1990.
4. D. Small. Simulating watercolor by modeling diffusion, pigment, and paper fibers. *Proc. of SPIE, Image Handling and Reproduction Systems Integration*, vol. 1460, 140–146, August 1991.
5. S. Schofield. *Non-photorealistic rendering: a critical examination and proposed system*. PhD thesis, School of Art and Design, Middlesex Univ., England, October 1993.
6. M.P. Salisbury, S.E. Anderson, R. Barzel, and D.H. Salesin. Interactive pen-and-ink illustration. *Proc. of SIGGRAPH '94*, 101–108, July 1994.
7. G. Winkenbach and D.H. Salesin. Computer-generated pen-and-ink illustration. *Proc. of SIGGRAPH '94*, 91–100, July 1994.
8. T. Strothotte, B. Preim, A. Raab, J. Schumann, and D.R. Forsey. How to render frames and influence people. *Computer Graphics Forum (Proc. of Eurographics'94)*, 13(3):455–466, August 1994.
9. P.M. Hall. Non-photorealistic shape cues for visualization. *Winter School of Computer Graphics, Univ. of West Bohemia, Plzen, Czech Republic*, 113–122, February 1995.

10. P. Decaudin. Cartoon-looking rendering of 3D-scenes. *INRIA, Syntim Research Group*, Research Report INRIA 2919, June 1996.
11. S.P. Worley. A cellular texturing basis function. *Proc. of SIGGRAPH '96*, 291–294, July 1996.
12. L. Markosian, M.A. Kowalski, S.J. Trychin, L.D. Bourdev, D. Goldstein, and J.F. Hughes. Real-time nonphotorealistic rendering. *Proc. of SIGGRAPH '97*, 415–420, August 1997.
13. C.J. Curtis, S.E. Anderson, J.E. Seims, K.W. Fleischer, and D.H. Salesin. Computer-generated watercolor. *Proc. of SIGGRAPH '97*, 421–430, August 1997.
14. S. Takagi and I. Fujishiro. Microscopic structural modeling of colored pencil drawings. *SIGGRAPH '97 Visual Proc.*, 187, August 1997.
15. G. Elber. Line art illustrations of parametric and implicit forms. *IEEE Trans. Visualization and Computer Graphics*, 4(1):71–81, January 1998.
16. A. Gooch. *Interactive Non-photorealistic Technical Illustration*. MSc thesis, Dept. of Computer Science, University of Utah, December 1998.
17. M.C. Sousa and J.W. Buchanan. Observational model of blenders and erasers in computer-generated pencil rendering. *Proc. of Graphics Interface '99*, 157–166, June 1999.
18. M.C. Sousa and J.W. Buchanan. Computer-generated graphite pencil rendering of 3D polygonal models. *Computer Graphics Forum (Proc. of Eurographics '99)*, 195–207, September 1999.
19. B. Maywood. *Personal communication*. Dept. Art and Design, University of Alberta, 1998.
20. A.L. Guptill. *Rendering in pencil*. Watson-Guption Publications Inc., New York (ISBN 0-8230-4531-5), 1977.
21. E.W. Watson. *Course in pencil sketching, four books in one*. Van Nostrand Reinhold Company, New York (ISBN 0-442-29230-9), 1978.
22. D. Lewis. *Pencil drawing techniques*. Watson-Guption Publications Inc., New York (ISBN 0-8230-3991-9), 1984.
23. G. Price. *Pencil drawing*. Crystal Productions (from the Art is... Video Series - SBN 1-56290-077-3), August 1993.
24. Parramon Editorial Team. *Barron's Art Handbooks Drawing*. Barron's Educational Series, Inc., New York (ISBN 0-7641-5007-3), 1997.
25. S.W. Camhy. *Art of the pencil: a revolutionary look at drawing, painting, and the pencil*. Watson-Guption Publications (ISBN 0-8230-1373-1), 1997.